

(triangular, rectangular, square, trapezoidal) and with various orientations of the [111] axis relative to the small faces of the slabs $\Delta z \Delta y$ which are parallel to the applied field. In all of these experiments the [111] axis determines the preferential orientation of the V lattice. However, the quality of the V crystal is best when the sample edges are aligned with the crystallographic lines of high density of the V lattice (as shown in the inset of Fig. 2). This indicates the effect of the faces parallel to the field on the preferential orientation of the V crystal along the anisotropy axis of the Nb crystal. This long-range influence arises as a consequence of the rigidity of the vortex lattice. The details of the experiments will be described later.⁸

We thank Professor J. Bok, Mr. J. M. Delrieu,

and Mr. R. Kahn for useful discussions and A. Guetta for his valuable technical assistance.

¹D. Cribier, B. Jacrot, L. Madhav Rao, and R. Farnoux, in *Progress in Low Temperature Physics*, edited by C. J. Gorter (North-Holland, Amsterdam, 1967), Vol. 5, p. 161.

²H. Trauble and U. Essmann, *Phys. Status Solidi* **18**, 813 (1966).

³Y. Simon and P. Thorel, *Phys. Lett.* **35A**, 450 (1971).

⁴J. M. Delrieu, *J. Low Temp. Phys.* **6**, 197 (1971).

⁵W. Fite and A. G. Redfield, *Phys. Rev. Lett.* **17**, 381 (1966).

⁶J. M. Delrieu and J. M. Winter, *Solid State Commun.* **4**, 545 (1966).

⁷A. Kung, *Phys. Rev. Lett.* **15**, 1006 (1970).

⁸P. Thorel, R. Kahn, Y. Simon, and D. Cribier, to be published.

Anisotropic Microstructure in Evaporated Amorphous Germanium Films*

G. S. Cargill, III

Department of Engineering and Applied Science, Yale University, New Haven, Connecticut 06520

(Received 20 March 1972)

Direct evidence for anisotropic microstructure in evaporated amorphous germanium films has been obtained from small-angle x-ray scattering. Low-density regions have approximate linear dimensions of 22 and 46 Å in the film plane and 2200 Å normal to the film plane for the 7- μ m-thick films studied. Their volume fraction is only 1 to 2%, if they are assumed to be voids.

Evaporated amorphous Ge and Si films are commonly less dense than crystalline films; the reported density deficits range from 0 to 30% and apparently depend on deposition conditions, as do many other properties of amorphous films.¹ This Letter presents results of small-angle x-ray scattering measurements which clarify the origin of such density deficits. Earlier electron² and x-ray³ scattering measurements indicated that most of the density deficit and its variation were associated with submicroscopic voids, rather than with the intrinsic amorphous structure. However, spherical or randomly oriented voids were assumed in interpreting the measurements.^{2,3} The present study indicates that evaporated amorphous germanium films (of $\sim 7 \mu\text{m}$ thickness) have anisotropic microstructures consisting of rodlike low-density regions oriented perpendicular to the film plane and that submicroscopic voids account for a much smaller part of the density deficit than previously thought. Galeener^{4,5} recently interpreted anomalous structure in uv dielectric constants of 1000-Å evaporated amor-

phous Ge films by postulating cracklike oriented voids. Donovan and Heinemann⁶ interpreted features in high-resolution electron micrographs of 100-Å films as voids of the type proposed by Galeener. The present results, on 7- μ m-thick films, indicate rodlike rather than cracklike voids.

The geometry used in the scattering measurements⁷ and the dependence of observed scattered intensity on both φ and K are shown in Fig. 1. Scattering is anisotropic for $K < 0.5 \text{ \AA}^{-1}$. Anisotropy is sharpest in the high-angle tail of the small-angle scattering, i.e., half-widths $\varphi_{1/2}$ are smallest here. The half-widths increase as the scattering angle is reduced. Absolute, slit-length-corrected intensities⁸ for $\varphi = 0$ are shown in Fig. 2 (squares) as $\log I$ versus K^2 .

These data were obtained for films which had been floated off their substrates in warm water or hydrofluoric acid. The large-angle x-ray scattering and radial distribution functions for these films are similar to those published elsewhere.^{2,3,9} Anisotropic small-angle scattering similar to

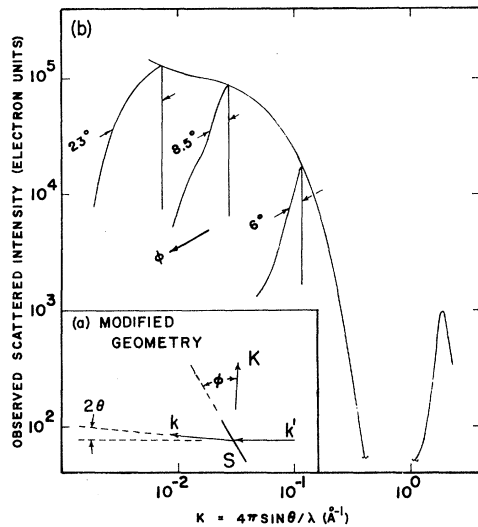


FIG. 1. (a) Modified scattering geometry; \vec{k}' is the incident beam direction, \vec{k} is the scattered beam direction, $\vec{K} = \vec{k} - \vec{k}'$; 2θ is the scattering angle; S is the planar sample; ϕ is the angle between \vec{K} and its projection in the plane of the sample. (b) Combined dependence of observed scattered intensity on both ϕ and K , with indicated half-widths at half-height.

that already described has also been found for films still on their substrates, although absolute intensity measurements have not yet been made for these films. Deposition conditions are summarized in Table I.

Measured intensities were well described as scattering by a collection of identical ellipsoids, with semiaxis lengths $A_1 \geq A_2 \geq A_3$. The A_1 axes were initially assumed to be normal to the plane of the film; A_2 and A_3 axes for different ellipsoids were randomly oriented in the film plane; and each ellipsoid was assumed to scatter independently. The ellipsoids represent rodlike ($A_1 \gg A_2 \sim A_3$) regions of less than or greater than bulk density, limiting cases being voids or regions of unusually dense packing.

Intensity profiles were calculated for this simple model in electron units per atom,^{10,11}

$$I_{eu}(K, \phi) = [\alpha V(\Delta\rho)^2 f^2 / \rho_0] (2/\pi) \times \int_0^{\pi/2} \Phi(KR(\phi, \xi)) d\xi, \quad (1)$$

where

$$\Phi(KR) = [3(\sin KR - KR \cos KR) / (KR)^3]^2, \quad (2)$$

$$R^2(\phi, \xi) = A_1^2 \sin^2 \phi + A_2^2 \cos^2 \phi \cos^2 \xi + A_3^2 \cos^2 \phi \sin^2 \xi, \quad (3)$$

α is the volume fraction of film occupied by these

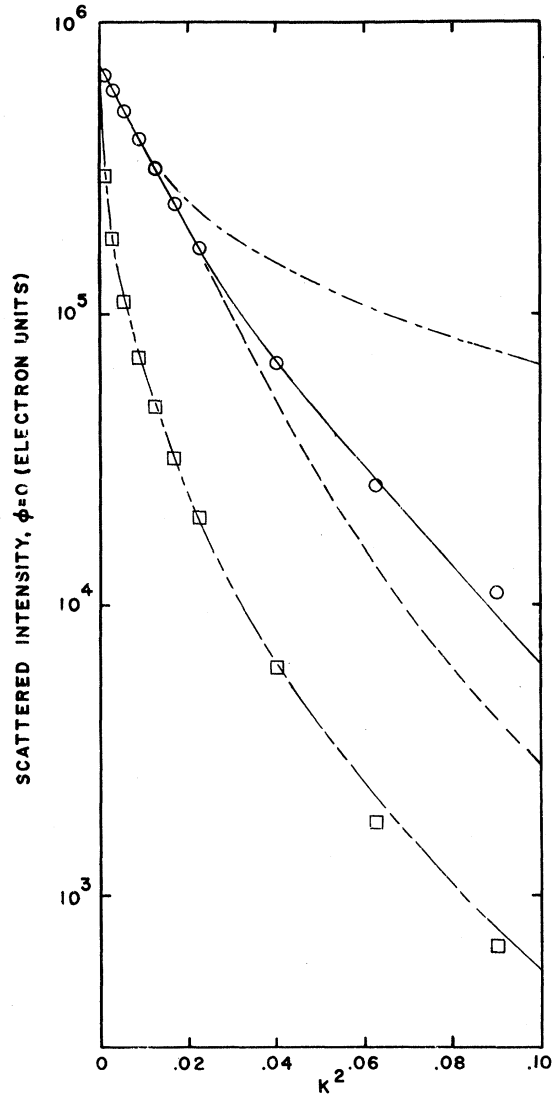


FIG. 2. Observed absolute, slit-length-corrected intensity for $\phi=0$ (squares); intensity corrected for 5° distribution width (circles); model calculations for $A_1 = 1100 \text{ \AA}$, with $A_2 = 22 \text{ \AA}$ and $A_3 = 12.8 \text{ \AA}$ (dashed curve), with $A_2 = 23 \text{ \AA}$ and $A_3 = 10.9 \text{ \AA}$ (solid curve), and with $A_2 = 25 \text{ \AA}$ and $A_3 = 4.8 \text{ \AA}$ (dot-dashed curve); and model calculation incorporating 5° distribution width for $A_1 = 1100 \text{ \AA}$, $A_2 = 23 \text{ \AA}$, and $A_3 = 10.9 \text{ \AA}$ (dash-double-dotted curve).

ellipsoidal regions, $V = (4\pi/3)A_1A_2A_3$, $\Delta\rho$ is the difference between the atomic density of the ellipsoidal regions and the average bulk density ρ_0 , and f is the atomic scattering factor.

The dependence of half-width $\phi_{1/2}$ on $1/K$ obtained from Eq. (1) is

$$\phi_{1/2}^{\text{model}}(\text{deg}) \approx \frac{180}{\pi} \frac{1}{K} \left(\frac{5 \ln 2}{A_1^2} \right)^{1/2} \quad (4)$$

when $\Phi(KR)$ is approximated by a Gaussian.¹⁰ As

TABLE I. Evaporated amorphous germanium films with anisotropic small-angle scattering.

Substrate material	Substrate temperature (°C)	Deposition rate (Å/sec)	Film thickness (μm)	Source to substrate distance (cm)	Vacuum during deposition (Torr)
Glass microscope slide ^a	100	5-10	7	25	10 ⁻⁵
1-mm silica glass ^b	50	50-75	4	19	10 ⁻⁷
0.2-mm Si [111] ^b	50	50-75	6	19	10 ⁻⁷
1-mm silica glass ^b	200	50-75	4	19	10 ⁻⁷

^aUsed after removal from substrates to obtain data in Figs. 1-3.

^bSupplied by A. H. Clark and studied without removal from substrates.

shown in Fig. 3, the data for $\varphi_{1/2}^{\text{observed}}$ versus $1/K$ can be fitted fairly well with a straight line, but with a positive intercept. This "distribution width" of 5° is attributed to anisotropic scattering regions not being perfectly aligned parallel to the film normal. The A_1 value obtained from these data with Eq. (4) was 1100 Å.

Values of A_2 and A_3 were obtained by comparing curves of $\log I$ versus K^2 , with $\varphi = 0$, for models and experiments. The experimental slit-length-corrected $\varphi = 0$ data were modified to correspond to zero distribution width by multiplying with $\varphi_{1/2}^{\text{obs}}(K)/\varphi_{1/2}^{\text{model}}(K)$. The modified scattering curve, Fig. 2 (circles), agrees well with the model calculation for $A_2 = 23$ Å and $A_3 = 10.9$ Å (solid line), indicating that regions which produce the anisotropic small-angle scattering are rod-shaped, the rod axes being nearly normal to the film plane.¹² Model curves for three choices of A_2, A_3 are shown. Results are also shown for a model calculation which incorporates the 5° distribution

width by appropriate Gaussian weighting of $\varphi \neq 0$ model curves.

Evaluation of Eq. (1) with $A_1 = 1100$ Å, $A_2 = 23$ Å, and $A_3 = 11$ Å for $K \rightarrow 0$ and extrapolation of the experimental curve of Fig. 2 to $K = 0$ yield

$$\alpha = \lim_{K \rightarrow 0} I_{eu}(K) \frac{1}{Vf^2} \frac{\rho_0}{(\Delta\rho)^2} = 1.6 \times 10^{-2} [1 - (\rho'/\rho_0)]^{-2}, \quad (5)$$

where ρ' is the density in the ellipsoidal regions and ρ_0 is the bulk density, assumed to be 10% less than the crystalline density.³ By limiting consideration to "two-phase" structures in which the scatters are deficient in density ($\rho' < \rho_0$) and in which they are surrounded by material no denser than crystalline germanium ($\rho_0 < \rho' \leq \rho_0^{\text{cryst}}$), only values of α less than ~30% are consistent with the scattering measurements. If the ellipsoidal regions are assumed to be voids, $\rho' = 0$ and $\alpha = 1.6\%$.

If the $\varphi = 0$ intensities were treated as isotropic

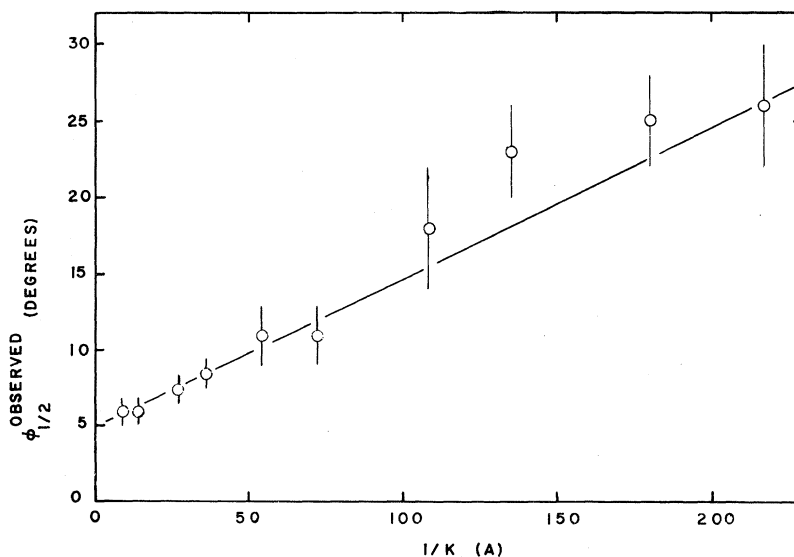


FIG. 3. Observed dependence of half-widths $\varphi_{1/2}$ on $1/K$.

small-angle scattering, α would be given by¹⁰

$$\alpha \approx (2\pi^2\rho_0 f^2)^{-1} \int K^2 I_{eu}(K) dK = 11\% \quad (6)$$

for $\rho' = 0$. This is between the values obtained by Shevchik and Paul³ for evaporated Ge (5%) and by Moss and Graczyk² for evaporated Si (10–15%) in assuming isotropic scattering. This qualitative agreement and the observation of anisotropic small-angle scattering from films prepared with a variety of evaporation conditions (see Table I) indicate that many films being used in experimental studies of electronic properties may be structurally anisotropic.

A much smaller part of the density difference between amorphous and crystalline forms of germanium can be attributed to well-defined internal voids, when Eq. (5) rather than Eq. (6) must be used in evaluating α . The amorphous film can no longer be thought of as a random network of essentially crystalline density but containing discrete voids which reduce its apparent density by approximating 10%.¹ The density deficit must be more uniformly distributed throughout the film volume.¹³

The present scattering data are inconsistent with the existence of cracklike voids of the type postulated by Galeener.⁵ Such voids would correspond to ellipsoids with $A_2 \gg A_3$. However, the data which he considered were obtained from films much thinner than those used in the present investigation. Clark and Burke¹⁴ recently found no anisotropy in electrical resistivity of evaporated amorphous germanium films from 0.4 to 4 μm thick. Deposition conditions were similar to those for the second entry in Table I. Their results can be reconciled either with low-density rodlike regions or with thin cracklike voids postulated by Galeener.¹⁵

The degree of anisotropy, dimensions, shapes, and volume fractions obtained in this study may not be representative of films prepared under different conditions. The effects of deposition parameters and subsequent annealing treatments on the anisotropic microstructure are currently being

studied.

The author is pleased to acknowledge technical assistance by V. Parisi and R. McGuire and useful discussions with N. J. Shevchik.

*Work supported in part by the National Science Foundation and Yale University.

¹H. Ehrenreich and D. Turnbull, *Comments Solid State Phys.* **3**, 75 (1970).

²S. C. Moss and J. F. Graczyk, *Phys. Rev. Lett.* **23**, 1167 (1969).

³N. J. Shevchik and W. Paul, in *Proceedings of the Fourth International Conference on Amorphous and Liquid Semiconductors*, Ann Arbor, Michigan, August 1971 (to be published).

⁴F. L. Galeener, *Phys. Rev. Lett.* **27**, 421 (1971).

⁵F. L. Galeener, *Phys. Rev. Lett.* **27**, 1716 (1971).

⁶T. M. Donovan and K. Heinemann, *Phys. Rev. Lett.* **27**, 1794 (1971).

⁷Complete experimental details including data handling will be discussed elsewhere.

⁸Measured intensities were corrected for slit-length smearing with a program by P. W. Schmidt, *Acta Crystallogr.* **19**, 938 (1965). Conversion to electron units per atom was accomplished by fitting to normalized large angle data in the 1.5–2.5 \AA^{-1} region.

⁹S. C. Moss and J. F. Graczyk, in *Proceedings of the Tenth International Conference on the Physics of Semiconductors*, Cambridge, Massachusetts, 1970, edited by S. P. Keller, J. C. Hensel, and F. Stern, CONF-700801 (U. S. AEC Division of Technical Information, Springfield, Va., 1970), p. 658.

¹⁰A. Guinier and G. Fournet, *Small-Angle Scattering of X-Rays* (Wiley, New York, 1955).

¹¹P. Mettelback and G. Porod, *Acta Phys. Austr.* **15**, 122 (1962).

¹²This is the simplest model which agrees with the measured intensities. Model structures with distributions of shapes, sizes, and orientations, but with the same autocorrelation function as the simple rod structure cannot be ruled out by scattering experiments.

¹³Present results do not rule out the possibility of a substantial density deficit due to monovacancies or divacancies.

¹⁴A. H. Clark and T. J. Burke, *Phys. Rev. Lett.* **28**, 678 (1972).

¹⁵A. H. Clark, private communication.